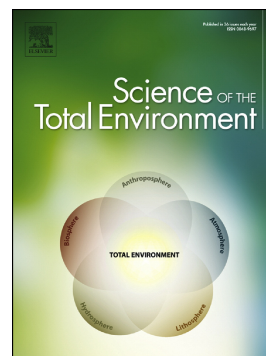


## Accepted Manuscript

Comparative study of atmospheric water-soluble organic aerosols composition in contrasting suburban environments in the Iberian Peninsula Coast

Regina M.B.O. Duarte, Maria Piñeiro-Iglesias, Purificación López-Mahía, Soledad Muniategui-Lorenzo, Jorge Moreda-Piñeiro, Artur M.S. Silva, Armando C. Duarte



PII: S0048-9697(18)33135-8  
DOI: doi:[10.1016/j.scitotenv.2018.08.171](https://doi.org/10.1016/j.scitotenv.2018.08.171)  
Reference: STOTEN 28233  
To appear in: *Science of the Total Environment*  
Received date: 23 April 2018  
Revised date: 26 July 2018  
Accepted date: 13 August 2018

Please cite this article as: Regina M.B.O. Duarte, Maria Piñeiro-Iglesias, Purificación López-Mahía, Soledad Muniategui-Lorenzo, Jorge Moreda-Piñeiro, Artur M.S. Silva, Armando C. Duarte , Comparative study of atmospheric water-soluble organic aerosols composition in contrasting suburban environments in the Iberian Peninsula Coast. Stoten (2018), doi:[10.1016/j.scitotenv.2018.08.171](https://doi.org/10.1016/j.scitotenv.2018.08.171)

This is a PDF file of an unedited manuscript that has been accepted for publication. As a service to our customers we are providing this early version of the manuscript. The manuscript will undergo copyediting, typesetting, and review of the resulting proof before it is published in its final form. Please note that during the production process errors may be discovered which could affect the content, and all legal disclaimers that apply to the journal pertain.

**Comparative study of atmospheric water-soluble organic aerosols composition  
in contrasting suburban environments in the Iberian Peninsula Coast**

Regina M.B.O. Duarte<sup>1\*</sup>, Maria Piñeiro-Iglesias<sup>2</sup>, Purificación López-Mahía<sup>2</sup>, Soledad Muniategui-Lorenzo<sup>2</sup>, Jorge Moreda-Piñeiro<sup>2</sup>, Artur M.S. Silva<sup>3</sup>, Armando C. Duarte<sup>1</sup>

<sup>1</sup> *Department of Chemistry & CESAM, University of Aveiro, 3810-193 Aveiro, Portugal*

<sup>2</sup> *Universidade da Coruña, Grupo Química Analítica Aplicada, Instituto Universitario de Medio Ambiente (IUMA), Centro de Investigaciones Científicas Avanzadas (CICA), Departamento de Química, A Coruña, Spain*

<sup>3</sup> *Department of Chemistry & QOPNA, University of Aveiro, 3810-193 Aveiro, Portugal*

*\*Corresponding author: E-mail: [regina.duarte@ua.pt](mailto:regina.duarte@ua.pt); Phone: +351 234370200.*

**Abstract:** This study investigates the structural composition and major sources of water-soluble organic matter (WSOM) from PM<sub>2.5</sub> collected, in parallel, during summer and winter, in two contrasting suburban sites at Iberian Peninsula Coast: Aveiro (Portugal) and Coruña (Spain). PM<sub>10</sub> samples were also collected at Coruña for comparison. Ambient concentrations of PM<sub>2.5</sub>, total nitrogen (TN), and WSOM were higher in Aveiro than in Coruña, with the highest levels found in winter at both locations. In Coruña, concentrations of PM<sub>10</sub>, TN, and WSOM were higher than those from PM<sub>2.5</sub>. Regardless of the season, stable isotopic  $\delta^{13}\text{C}$  and  $\delta^{15}\text{N}$  in PM<sub>2.5</sub> suggested important contributions of anthropogenic fresh organic aerosols (OAs) at Aveiro. In Coruña,  $\delta^{13}\text{C}$  and  $\delta^{15}\text{N}$  of PM<sub>2.5</sub> and PM<sub>10</sub> suggests decreased anthropogenic input during summer. Although excitation-emission fluorescence profiles were similar for all WSOM samples, multi-dimensional nuclear magnetic resonance (NMR) spectroscopy confirmed differences in their structural composition, reflecting differences in aging processes and/or local sources between the two locations. In PM<sub>2.5</sub> WSOM in Aveiro, the relative distribution of non-exchangeable proton functional groups was in the order: H-C (40-43%) > H-C-C= (31-39%) > H-

C-O (12-15%) > Ar-H (5.0-13%). However, in PM<sub>2.5</sub> and PM<sub>10</sub> WSOM in Coruña, the relative contribution of H-C-O groups (24-30% and 23-29%, respectively) equals and/or surpasses that of H-C-C= (25-26% and 25-29%, respectively), being also higher than those of Aveiro. In both locations, the highest aromatic contents were observed during winter due to biomass burning emissions. The structural composition of PM<sub>2.5</sub> and PM<sub>10</sub> WSOM in Coruña is dominated by oxygenated aliphatic compounds, reflecting the contribution of secondary OAs from biogenic, soil dust, and minor influence of anthropogenic emissions. In contrast, the composition of PM<sub>2.5</sub> WSOM in Aveiro appears to be significantly impacted by fresh and secondary anthropogenic OAs. Marine and biomass burning OAs are important contributors, common to both sites.

**Keywords:** Water-soluble organic aerosols; Suburban environments; Chemical and source signatures; NMR spectroscopy; Stable isotopic ( $\delta^{13}\text{C}$ ,  $\delta^{15}\text{N}$ ) composition; Water-soluble trace metals

## 1. Introduction

The study of the water-soluble fraction of organic aerosols (OAs) has been in the spotlight of atmospheric research community due to its effects on aerosol optical depth (Andreae and Gelencsér, 2006; Mladenov et al., 2010; Moise et al., 2015), cloud formation and properties (Martin et al., 2013; Padró et al., 2010; Sun and Ariya, 2006; Wonaschütz et al., 2013), radiation balance (Bond et al., 2013; Laskin et al., 2015; Moise et al., 2015), and atmospheric chemistry (George et al., 2015; Laskin et al., 2015; Mellouki et al., 2015). Atmospheric deposition (wet and dry) is the major pathway for removal of organic carbon (OC) from the atmosphere, thus affecting both atmospheric and land processes, particularly in sensitive ecosystems [e.g., (Witkowska et al., 2016; Witkowska and Lewandowska, 2016; Xie et al., 2016)]. Exposure to OAs has been also linked to a wide range of adverse health effects (e.g., cardiovascular diseases and respiratory problems) (Pöschl, 2005), with many of these toxic effects being attributed to the oxidative or oxidant generating properties of water-soluble organic constituents (Saffari et al., 2014; Verma et al., 2014). Yet, the ability to address the fundamental issues

associated with atmospheric chemistry dynamics, climate, and health impact of the water-soluble OAs is limited, mostly because the molecular complexity of aerosol water-soluble organic matter (WSOM) has hindered routine identification of its constituents. Moreover, a myriad of emission sources (natural and anthropogenic) and formation/aging mechanisms (secondary OAs) contribute significantly to the aerosol WSOM burden (Pöschl, 2005), further complicating the molecular characterization of this OAs component.

In Northern Hemisphere midlatitudes, the organic matter may account for 18-70% of tropospheric submicron particulate matter (Zhang et al., 2007), whereas lower percentage values have been reported for Southern Hemisphere locations [e.g., (Duarte et al., 2017b)]. In Europe, the organic matter is also the major single component (15-26%) of both fine and coarse particulate matter ( $PM_{2.5}$  and  $PM_{10}$ , respectively), with the highest loads being recorded at urban and traffic sites (Putaud et al., 2010). In Southern European regional background and suburban sites, the total carbonaceous fraction [organic matter plus elemental carbon (EC)] is also an important aerosol component, contributing to 28-41% of  $PM_{2.5}$  (Duarte et al., 2017a; Pio et al., 2007; Querol et al., 2013, 2009). Notwithstanding these relatively high proportions in ambient PM, the molecular features and source contributions of OAs, including their water-soluble organic component, are still not fully understood. Furthermore, it is also important to note that the water-solubility of OAs from different sources is different [e.g., (Xu et al., 2017)]. Therefore, assessing the water-solubility of ambient OAs and their major structural features would provide not only a better constrain on the types of compounds emitted and/or formed in the atmosphere, but also an in-depth understanding of the contribution from different sources to ambient OAs.

Within Southern Europe, the atmosphere at the Western European Coast supports multiple man-made (e.g., urban, industrial, shipping, and agricultural activities) and climatic (e.g., atmospheric circulation from North Atlantic) stressors with clear socio-economic impacts (Ramos et al., 2016; Russo et al., 2018). As such, the source contributions of OAs at this region are likely to include both primary (sea spray, mineral dust, fossil fuel combustion, wood burning) and secondary (e.g., atmospheric aging and photooxidation) sources (Duarte et al., 2017a, 2015; García-Santiago et al., 2017; Gómez-Carracedo et al., 2015; Lopes et al., 2015; Matos et al., 2017; Moreda-Piñeiro et al., 2015; Viana et al., 2008). However, important questions still remain: (i) how the levels of ambient OAs, in particular of the water-soluble organic fraction,

distribute along this region located at the land-sea interface, (ii) how they compare in terms of their structural composition and sources, and (iii) whether would be possible to potentially complement existing OAs source profiles within this region. Hence, this study aims at addressing these three questions, using a multidimensional non-targeted analytical approach (Matos et al., 2017, 2015a), based on one-dimensional (1D) and two-dimensional (2D) solution-state nuclear magnetic resonance (NMR) and excitation-emission matrix (EEM) fluorescence spectroscopies, to investigate the structural composition and major sources of the WSOM from  $PM_{2.5}$  samples collected, simultaneously, during summer and winter, in two different suburban sites at the Iberian Peninsula Coast: Aveiro (Portugal) and A Coruña (Spain).  $PM_{10}$  samples were also collected concomitantly at A Coruña for comparing and complement the dataset on the main structural features and sources of aerosol WSOM in this suburban location. Stable isotopic ( $\delta^{13}C$  and  $\delta^{15}N$ ) and water-soluble trace metals compositions of the bulk  $PM_{2.5}$  and  $PM_{10}$  samples were also assessed to better understand the contribution of various sources to OAs at the studied locations.

## **2. Materials and methods**

### **2.1. Aerosol samples collection**

In Aveiro, with approximately 60,000 inhabitants, the aerosol sampling occurred at the Campus (Santiago) of the University of Aveiro, on a rooftop approximately 20 m above the ground. The sampling site is located on the west coast of Portugal, 10 km from the Atlantic Ocean, and very close to the city center [Figure S1, section S1, in Supporting Information (SI)]. An industrial complex, which includes the production of nitric acid, aniline, nitrobenzene and chlorinate compounds, is located 15 km to the North of Aveiro. A Coruña is a coastal city in the northwest of Spain with a quarter of a million inhabitants. The aerosol measurements were carried out at the urban background site (Oleiros) located near the sea (~0.8 km), and near the neighboring city of A Coruña (located at 8 km) [Figure S1, section S1, in SI]. The sampling site is close to a residential area, and in immediate vicinity is agricultural lands, forests and the sea. The main anthropogenic sources are the emissions from traffic and domestic activities, but also industrial emissions can influence air quality in the study area. Because of its proximity to the sea, the

local wind pattern is mainly driven by the land-sea breeze. North-westerly synoptic winds are dominant and generally carry relatively clean air from the sea, but other wind directions are also recorded, with a significant contribution to air pollution levels at this site.

In both sampling locations, a total of eight high-volume  $PM_{2.5}$  samples (particles with aerodynamic diameter less than  $2.5 \mu m$ ) were simultaneously collected on quartz fibre filters, on a weekly basis (7 days in continuum), during September–October 2016 [ $n = 4$ , Summer (SU2016)] and January–February 2017 [ $n = 4$ , Winter (WI2017)] in order to collect enough material for subsequent WSOM characterization. In A Coruña, eight high-volume  $PM_{10}$  samples (particles with aerodynamic diameter less than  $10 \mu m$ ) were concomitantly collected in both seasons, following the same sampling procedure. One field blank was collected in each sampling period in order to correct for ambient background  $PM_{2.5}$  and  $PM_{10}$  mass, total carbon (TC), water-soluble organic carbon (WSOC), total nitrogen (TN), isotopic ( $\delta^{13}C$  and  $\delta^{15}N$ ), and water-soluble trace metals levels. This sampling procedure is similar to those adopted in previous studies of advanced structural characterization of aerosol WSOM from low sample size groups (Duarte et al., 2015; Duarte et al., 2017b; Duarte et al. 2005; Duarte et al., 2007; Duarte et al., 2008; Lopes et al., 2015; Matos et al., 2017; Matos et al., 2015b). Additional details on aerosol sampling procedure in Aveiro and A Coruña are available in section S1, in SI. After sampling, filter samples were folded in two, with the exposed side face to face, wrapped in aluminum foil and immediately transported to the laboratory in charge of the sampling site, where they were weighted and stored frozen (up to 6 months) until further analysis (section S1, SI). The sampled filters and filter blanks were divided into two fractions, enclosed into heated treated aluminum foil, and one of the fractions were sent by express mail to the laboratories participating in this study.

## **2.2. Extraction and determination of WSOC in aerosol samples**

Depending on the available filter area, the volume of ultra-pure water used for the extraction of WSOC had to be adjusted in order to comply with a “filter area-to-water volume ratio” of  $1.2 \text{ cm}^2 \text{ mL}^{-1}$ . This ratio was set based on the work of Salma et al. (2007), being a well-established value for the quantitative extraction of the WSOC from atmospheric particles deposited onto quartz filters. For the aerosol samples collected in Aveiro, each quartz filter was

extracted with 150 mL of ultra-pure water (18.2 M $\Omega$  cm) by mechanical stirring for 2 min followed by ultrasonic bath for 15 min. This same extraction methodology was applied to the aerosol samples collected in A Coruña using a volume of ultra-pure water of 75 mL. Each final aqueous slurry was filtered through a hydrophilic polyvinylidene fluoride (PVDF) membrane filter (Durapore<sup>®</sup>, Millipore, Ireland) of 0.22  $\mu$ m pore size. At the end of this filtration step, the slurry residue was washed twice with 5 mL of ultrapure water in order to remove any WSOC still loosely bound to the filter residues. At least two different blanks were performed for each of extractions. Concentrations of blanks were below the detection limits. Also, to avoid metal contamination during filters pretreatment and analysis, all plastic ware and glassware were washed with ultrapure water of 18 M $\Omega$  cm resistance and kept for 48 h in 10% (v/v) nitric acid (ultraclean nitric acid 69–70 %), and then rinsed several times with ultrapure water before use. After collection, sample manipulation and analysis were carried out in a class-100 clean room. The dissolved organic carbon (DOC) content of each aqueous aerosol extract was measured with a Skalar (Breda, Netherlands) San++ Automated Wet Chemistry Analyzer, based on a UV-persulfate oxidation method. The WSOC concentrations are expressed in  $\mu$ g C m<sup>-3</sup>.

After WSOC extraction, small aliquots of each PM<sub>2.5</sub> and PM<sub>10</sub> aqueous extract was withdrawn for EEM fluorescence (section 2.3) and water-soluble trace metals (section 2.4) analyses. Afterwards, and to ensure enough mass for the structural characterization, the aqueous extracts were batched together into four WSOM samples, representative of each suburban location and season (Aveiro – SU2016; Aveiro – WI2017; A Coruña – SU2016; A Coruña – WI2017). Each pooled WSOC sample analyzed in this study was concentrated under rotary evaporation followed by a freeze-drying procedure and kept on a desiccator over silica gel until NMR analysis (section 2.5).

### **2.3. EEM fluorescence spectroscopy**

The EEM fluorescence spectrum of each PM<sub>2.5</sub> and PM<sub>10</sub> aqueous extract was recorded on a spectrophotometer JASCO (Tokyo, Japan), model FP-6500 using a 1 cm path-length quartz cuvette. Excitation and emission wavelength ranges were set from 220 to 450 nm and 250 to 600 nm, respectively, and their scanning intervals were set at 10 nm and 5 nm, respectively. The excitation and emission slit widths were fixed at 10 nm and the scan speed was set at

100 nm/min. For each day of analysis, a spectrum of a sample of ultra-pure water was acquired under the same experimental conditions and used as blank.

#### **2.4. Water-soluble trace metal analysis**

Water soluble metals in PM<sub>2.5</sub> and PM<sub>10</sub> aqueous extracts (section 2.2) were analyzed by inductively coupled plasma–mass spectrometry (ICP-MS), Thermo Finnigan X Series (Waltham, 125 MA, USA). Optimal conditions for ICP-MS were as follows: radio frequency (RF) power 1360 W, nebuliser gas flow 0.9 L min<sup>-1</sup>, auxiliary gas flow 0.9 L min<sup>-1</sup>, and plasma gas flow 15.0 L min<sup>-1</sup>. Detection was performed in the peak jump mode; monitored ions were m/z 27, 75, 137, 44, 111, 59, 52, 65, 56, 39, 24, 55, 95, 23, 60, 208, 51 and 64 for Al, As, Ba, Ca, Cd, Co, Cr, Cu, Fe, K, Mg, Mn, Mo, Na, Ni, Pb, V and Zn, respectively. Calibrations were based on 2.0 M nitric acid aqueous standard solutions covering metal concentrations from 0 to 500 µg L<sup>-1</sup>. Yttrium and indium (5.0 µg L<sup>-1</sup>), germanium (10.0 µg L<sup>-1</sup>), and scandium (50.0 µg L<sup>-1</sup>) were selected as internal standards. Trueness of the method was assessed by analyzing WS-PE trace Metals Mix from AccuStandard (New Haven, CT, USA).

#### **2.5. Solution-state 1D and 2D NMR spectroscopy**

All NMR spectra were acquired using a Bruker Avance-500 spectrometer operating at 500.13 and 125.77 MHz for <sup>1</sup>H and <sup>13</sup>C, respectively, and equipped with a liquid nitrogen cooling CryoProbe Prodigy™. All 1D and 2D spectra were run at 295.1 K, and additional details on NMR data acquisition can be found in Section S2, in SI. The dried WSOM samples were dissolved in deuterated methanol (MeOH-*d*<sub>4</sub>, ~1 mL) and transferred to 5 mm NMR tubes. The identification of functional groups in the NMR spectra was based on their chemical shift relative to the central solvent (MeOH-*d*<sub>4</sub>) peak set at δ<sub>H</sub> 3.31 ppm and δ<sub>C</sub> 49.0 ppm. The interpretation of the spectral regions and structural assignments were based on the NMR chemical shift data described in the literature for standard organic compounds and for natural organic matter (NOM) from different environmental matrices (Duarte et al., 2008; Hertkorn and Kettrup, 2005; Lopes et al., 2015; Matos et al., 2017; Simpson et al., 2001), as well as on data generated by NMR simulators software's and databases (namely, Perkin Elmer ChemBioDraw® Ultra 14.0 and nmrdb.org (Banfi and Patiny, 2008)).

## 2.6. Stable isotopic $\delta^{13}\text{C}$ and $\delta^{15}\text{N}$ analysis

Carbon ( $\delta^{13}\text{C}$ ) and nitrogen ( $\delta^{15}\text{N}$ ) isotopes analysis was performed using a stable Isotope Ratio Mass Spectrometer (IRMS) calibrated by international certified reference standards (NBS-22, IAEA-CH-6 and USGS 24) by International Atomic Energy Agency (Vienna, Austria). The filters were analyzed with an elemental analyzer FlashEA 1112 connected to the stable isotope ratio mass spectrometer Thermo Finnigan Delta Plus through a ConFlo II interface. Two small discs (diameter 0.9 cm) were placed into the tin capsule and combusted in the oxidation furnace at the temperature of the 1020° C in excess of oxygen. Later this gas was transferred into the reduction furnace (650° C) and separated by a GC column (40° C). The precision (standard deviation) for the analysis of  $\delta^{13}\text{C}$  and  $\delta^{15}\text{N}$  of the laboratory standard (acetanilide) was  $\pm 0.15$  ‰ (1-sigma, n=10). The analysis comprised evaluation of the  $^{13}\text{C}$  to  $^{12}\text{C}$  or  $^{15}\text{N}$  to  $^{14}\text{N}$  isotope ratios, expressed as  $\delta$  (delta) values and defined as the standard-normalized difference from the reference standard, and expressed as  $\delta^{13}\text{C}$  or  $\delta^{15}\text{N}$  in parts per mill (‰).

## 3. Results and discussion

### 3.1. Mass concentrations of TC, TN, and WSOC in ambient particulate matter

Table 1 reports the range and median values of ambient concentrations of PM, TC, TN, WSOC, total mass of particulate WSOM, and percentage of mass ratio between WSOM and PM at each studied location. The ambient concentrations of TC and TN were estimated based on isotopic  $\delta^{13}\text{C}$  and  $\delta^{15}\text{N}$  data, respectively. The total mass of WSOM was estimated as  $1.6 \times \text{WSOC}$ , based on elemental analysis performed on the WSOC aerosol samples collected at Aveiro (Duarte et al., 2015). In Aveiro, this factor ranged between 1.5 in winter and 1.7 in summer, yielding an average WSOM-to-WSOC ratio of 1.6 (Duarte et al., 2015). It is very likely that this ratio would vary from site to site; however, due to the lack of additional information for the region of A Coruña, a value of 1.6 was used here to calculate the total mass of particulate WSOM at both sites.

<TABLE 1>

As depicted in Table 1, the ambient concentrations of  $PM_{2.5}$  and its TC and WSOC components were consistently higher in Aveiro than in A Coruña, with the highest levels being found during the winter season at both locations. This seasonal trend has been already quite well documented in this and other regions (Duarte et al., 2017b, 2015, 2007; Kiss et al., 2002; Shakya et al., 2012), although an opposite trend has been observed in North America [e.g., (Park et al., 2003; Wozniak et al., 2012)]. Moreover, in summer, the contribution of WSOC to TC in  $PM_{2.5}$  is higher in Aveiro than in A Coruña, whereas in winter, the WSOC/TC ratios are of same order of magnitude in both locations and higher than those found during warmer conditions. The scatter plot of WSOC *versus* TC in  $PM_{2.5}$  [Figure 1(a)] also indicates a relationship between these two carbonaceous fractions, which is higher in Aveiro ( $R^2 = 0.84$ ,  $n = 8$ ) than in A Coruña ( $R^2 = 0.54$ ,  $n = 8$ ). In Aveiro, this trend suggests that both TC and its water-soluble organic fraction are probably derived from the same primary emission source(s) and/or are influenced by similar secondary processes in the atmosphere. In previous studies carried out at this suburban site, it has been shown that contributions of biomass burning combined with less warm weather conditions (favoring the particulate phase of semi-volatile organics) are important contributors to ambient TC and water-soluble OA levels during winter [e.g., (Duarte et al., 2017b, 2015; Lopes et al., 2015; Matos et al., 2017)]. In summer, secondary OAs from fossil fuel combustion may prevail over primary sources as an important contributor to fine particulate TC and WSOC fractions (Lopes et al., 2015). In A Coruña, on the other hand, the large spread of WSOC/TC ratios in  $PM_{2.5}$  (8.1 to 46%, Table 1), combined with the low correlation between WSOC and TC, and low ambient concentrations of  $PM_{2.5}$ , TC, and WSOC further suggests dissimilar seasonal and spatial variability in emission sources, their strength, and contribution from aging processes at this suburban site. Interestingly, the range and median values of the WSOC/ $PM_{2.5}$  ratio (Table 1) are rather similar between the two coastal locations regardless of the seasonal period, with the highest values being again found during winter. This finding suggests that the mass contribution of the WSOC fraction to  $PM_{2.5}$  do not portray the differences in specific water-soluble organic compounds and their sources which were identified in these two locations (additional details in section 3.4).

<FIGURE 1>

Publications describing WSOC concentrations in aerosols are most often concentrated on PM<sub>2.5</sub> size-range. When the size distribution of WSOC is discussed [e.g., (Contini et al., 2014; Witkowska and Lewandowska, 2016)], this carbonaceous fraction is typically dominant in the size interval up to 2.5 µm. In aerosols collected in A Coruña, the particulate matter in suspension is enriched in PM<sub>10</sub> coarse fraction (i.e., particles with aerodynamic diameter between 2.5 and 10 µm), especially during summer (Table 1). While during the warmer period the PM<sub>2.5</sub> size-fraction comprised only 27-37% of the PM<sub>10</sub>, during winter the fine-size fraction represented 39-41% of the PM<sub>10</sub>. In a similar vein, the highest levels of TC and WSOM were comprised in the PM<sub>10</sub> coarse fraction in both seasons. The ranges of PM<sub>2.5</sub>/PM<sub>10</sub> ratios for TC and WSOM were as follows: TC: 33-49% and 33-44%, and WSOM: 29-34% and 39-42% during summer and winter season, respectively. These findings also indicate an apparent increase on the contribution of the WSOM component for the fine size-range particles during winter, thus suggesting an enhanced contribution of primary emission sources of fine water-soluble OAs [e.g., biomass burning (Duarte et al., 2017b, 2015; Lopes et al., 2015; Matos et al., 2017)] and/or aging of these compounds in the colder season. The scatter plot of WSOC *versus* TC in both aerosol size fractions [Figure 1(b)] further indicates a better correlation between these two carbonaceous fractions in coarse PM<sub>10</sub> ( $R^2 = 0.65$ ,  $n = 8$ ) than in PM<sub>2.5</sub> ( $R^2 = 0.54$ ,  $n = 8$ ) samples. This feature suggests that both TC and WSOC in PM<sub>10</sub> coarse fraction are being influenced by similar emission sources [e.g., biomass burning (Reid et al., 2005)] and local conditions, particularly during the winter season, whereas their presence in PM<sub>2.5</sub> may be influenced by different emission sources and/or removal processes.

The TN content at each studied location (Table 1) had a narrow range of variation in PM<sub>2.5</sub> samples, with the highest values being found in Aveiro during both seasons. These findings may be due to differences both in the emission of nitrogenous gaseous precursors and photochemical atmospheric processes taking place in the studied locations. The TC/TN weight ratios in PM<sub>2.5</sub> samples collected in Aveiro ranged from 2.1 to 6.6 (median: 4.1) in summer and from 5.4 to 12 (median: 8.3) in winter, whereas in A Coruña the TC/TN ratio ranged from 7.4 to 8.8 (median: 7.9) in summer and from 6.8 to 11 (median: 7.9) in winter. A strong positive correlation between TN and TC in both PM<sub>2.5</sub> ( $R^2 = 0.95$ ,  $n = 8$ ) and PM<sub>10</sub> ( $R^2 = 0.96$ ,  $n = 8$ ) samples from A Coruña may indicate that TC and TN have a common source in both aerosol

size fractions during both seasons. On the other hand, a somewhat lower correlation between TN and TC ( $R^2 = 0.62$ ,  $n = 8$ ) in  $PM_{2.5}$  samples collected in Aveiro, suggest that these two aerosol components originate from different sources during both seasons at this coastal location.

### **3.2. Water-soluble metals and isotopic $\delta^{13}C$ and $\delta^{15}N$ composition of ambient particulate matter**

Table 2 shows the results of isotopic  $\delta^{13}C$  and  $\delta^{15}N$  composition in the fine and coarse fractions during winter and summer season samplings in Aveiro and A Coruña. The highest median  $\delta^{13}C$  values were found in the  $PM_{2.5}$  and  $PM_{10}$  samples collected in A Coruña during the warmer period. These samples also exhibit the lowest median  $\delta^{15}N$  values. Previous studies on stable isotopic  $\delta^{13}C$  of TC in atmospheric aerosols at different locations (urban, rural, and pristine) have shown that the  $\delta^{13}C$  values of anthropogenic carbonaceous aerosols range between -27 to -25‰, with the lowest and highest values being associated with anthropogenic fresh and aged aerosols, respectively (Aggarwal et al., 2013; Mkombe et al., 2014; Narukawa et al., 2008). The examples discussed in the literature suggest that the isotopic  $\delta^{13}C$  data obtained in A Coruña during summer are consistent with the values obtained when the particulate matter is relatively aged (i.e., photochemically more processed) and less influenced by anthropogenic emissions of fresh OAs. On the other hand, the low values during the colder period could be explained by (1) changes in the contribution of OAs sources, and (2) less photochemical activities with concomitant enhancement of gas-to-particle processes. These two factors could also explain the isotopic enrichment of  $\delta^{15}N$  in both  $PM_{2.5}$  and  $PM_{10}$  samples collected in A Coruña during winter. The lower  $\delta^{15}N$  values during summer in A Coruña could also hint a higher contribution of marine nitrogen species (with lighter  $\delta^{15}N$ ) at this suburban location (Agnihotri et al., 2015). Indeed, throughout the summer campaign at A Coruña, the backward air masses trajectories are mostly characterized by air masses that traveled over the Atlantic Ocean (Table S1, Section S3, in SI). On the other hand, regardless of the seasonal period, the isotopic  $\delta^{13}C$  and  $\delta^{15}N$  data obtained in Aveiro may be mainly associated with the presence of anthropogenic fresh OAs.

<TABLE 2>

Water-soluble metal contents in  $PM_{2.5}$  and  $PM_{10}$  collected in Aveiro and A Coruña during winter and summer seasons are shown in Table S2 (Section S4, in SI).  $Na^+$  dominates the cation budget with the sequence  $Na^+ > K^+ > Ca^{2+} \sim Mg^{2+}$  in Aveiro and A Coruña. The highest soluble trace metal concentrations were registered for Al, Fe and Zn. On the other hand, As, Cd, Co and Mo offers the lowest values. Results shown in Table S2 are generally in good agreement with reported values for water-soluble metals at coastal sites (Moreda-Piñeiro et al., 2015). Water-soluble metal content is generally impacted by the particulate matter origin (see principal component and cluster analysis in Section S5, in SI).

### **3.3. Fluorescence properties of aerosol WSOM**

Figure 2 shows typical EEM fluorescence profiles of WSOM in atmospheric aerosol samples collected in Aveiro and A Coruña during summer and winter seasons. Two common fluorophores were found in most of the EEM profiles: fluorophores  $\alpha$  (excitation/emission maxima at 240-250/410-420 nm) and  $\alpha'$  (excitation/emission maxima at 310-320/410-420 nm). Fluorescence profiles similar to those of fluorophores  $\alpha$  and  $\alpha'$  are already well documented for natural organic matter (NOM) samples from different environmental matrices (Andrade-Eiroa et al., 2013; Bagtho et al., 2011; Singh et al., 2010; Stedmon et al., 2003), including also WSOM from atmospheric aerosols (Chen et al., 2016; Duarte et al., 2004; Fan et al., 2016; Fu et al., 2015; Matos et al., 2015a; Mladenov et al., 2011). These two WSOM fluorophores are usually associated with humic-like materials of terrestrial and aquatic origin (Chen et al., 2016; Fan et al., 2016; Fu et al., 2015; Mladenov et al., 2011). However, one should be careful when associating the spectral features of these fluorophores to those of humic-like substances occurring in water and soils, since these are unlikely to resemble the WSOM from atmospheric aerosols, both in origin/transformation and compositional terms (Duarte et al., 2007; Matos et al., 2015a). In fact, fluorophore  $\alpha'$  is also similar to the peaks in the EEM profiles of secondary OAs from the ozonolysis of  $\alpha$ -pinene (Lee et al., 2013). This difficulty in assigning fluorophores  $\alpha$  and  $\alpha'$  to specific organic species indicates that a final conclusion on the structural nature of the whole aerosol WSOM samples cannot be withdrawn based solely on their EEM fluorescence profiles.

<FIGURE 2>

The spatial and temporal variations of the intensity of fluorophores  $\alpha$  and  $\alpha'$  seems to be also consistent with those of TC and WSOC, with the highest intensities being found for PM<sub>2.5</sub> samples collected in Aveiro during the winter season. Of notice, the remarkable decrease in the intensity of fluorophore  $\alpha$  in the EEM spectra of PM<sub>10</sub> samples collected in A Coruña during winter. The fluorescence feature of PM<sub>10</sub> samples in winter resemble that of WSOM from diesel exhaust particles (Mladenov et al., 2011), being consistent with the isotopic  $\delta^{13}\text{C}$  and  $\delta^{15}\text{N}$  data, which suggest a higher influence of anthropogenic emissions of fresh OAs during this period at this Spanish location.

### 3.4. Structural and molecular characterization of aerosol WSOM

The solution-state 1D  $^1\text{H}$  NMR spectra of the WSOM from PM<sub>2.5</sub> and PM<sub>10</sub> samples collected at the two suburban locations are illustrated in Figures 3(a) to 3(f). All spectra consist of a complex overlapping profile with broad bands superimposed by a relatively small number of sharp peaks. Although a very limited number of resonances can be assigned to specific organic compounds, four main categories of functional groups carrying C-H bonds can be identified in these  $^1\text{H}$  NMR spectra: (i)  $\delta$   $^1\text{H}$  0.5–1.9 ppm – protons bound to carbon atoms of straight and branched aliphatic chains (H-C), which includes protons from methyl (R-CH<sub>3</sub>), methylene (R-CH<sub>2</sub>), and methyne (R-CH) groups; (ii)  $\delta$   $^1\text{H}$  1.9–3.2 ppm – protons bound to carbon atoms in  $\alpha$ -position to unsaturated groups in allylic (H-C <sub>$\alpha$</sub> -C=), carbonyl or imino (H-C <sub>$\alpha$</sub> -C=O or H-C <sub>$\alpha$</sub> -C=N) groups, protons from methyl groups bound to an aromatic carbon, and protons in secondary and tertiary amines (H-C-NHR and H-C-NR<sub>2</sub>); (iii)  $\delta$   $^1\text{H}$  3.5–4.1 ppm – protons bound to oxygenated saturated aliphatic carbon atoms (H-C-O) in alcohols, polyols, ethers, esters, and organic nitrate (R-CH<sub>2</sub>-O-NO<sub>2</sub>), and (iv)  $\delta$   $^1\text{H}$  6.5–8.3 ppm – protons bound to aromatic carbon atoms (Ar-H). Additional NMR resonances at  $\delta$   $^1\text{H}$  5.0–5.3 ppm, assigned to protons bound to anomeric carbons [O-C(H)-O], can be also distinguished in all spectra.

<FIGURE 3>

For a further understanding of the  $^1\text{H}$  NMR spectra profiles, a quantitative integration of the four main spectral regions was performed in order to assess the abundance of each functionality in the WSOM samples. As depicted in Figure 3(g), regardless of the studied environment, all aerosol WSOM samples exhibit the same major proton types; however, they differ in terms of

the relative distribution of the major proton regions. Overall, the relative content of the proton functional groups obtained in this study are within the range of those published for aerosol WSOM samples from urban, rural, forest, and coastal environments (e.g., (Chalbot et al., 2016, 2014; Decesari et al., 2005; Duarte et al., 2017b; Graham et al., 2002; Lopes et al., 2015; Song et al., 2012). For the WSOM samples collected in Aveiro, the relative contributions of the four proton functional groups exhibits the following typical variation: H-C (40-43%) > H-C-C= (31-39%) > H-C-O (12-15%) > Ar-H (5.0-13%). However, a different trend is observed for PM<sub>2.5</sub> and PM<sub>10</sub> samples collected in A Coruña, for which the relative contribution of H-C-O structures (24-30% and 23-29%, respectively) equals (or surpasses, as in the case of winter samples) that of the H-C-C= structures (25-26% and 25-29%, respectively), being also higher than those of the PM<sub>2.5</sub> samples collected in Aveiro. Examples of organic species that typically resonate in the H-C-O region includes sugar alcohols (e.g., mannitol and arabitol), carbohydrate-like moieties (e.g., glucose, sucrose, fructose), and some anhydrosugars such as levoglucosan and mannosan) (Chalbot et al., 2016, 2014; Duarte et al., 2008; Matos et al., 2017). Sugar alcohols are molecular tracers for fungal spores from vegetation [e.g., (Bauer et al., 2008; Fu et al., 2012, 2010; Liang et al., 2013)], as well as decomposing plants during cold seasons (Burshtein et al., 2011). Their presence in aerosol WSOM collected in A Coruña is consistent with the characteristics of the sampling site, which is surrounded by vegetation, and it represents a suburban scenario with low influence of emissions from industrial and traffic sources. Moreover, primary saccharides can have a biological origin [e.g., (Fu et al., 2010)], whereas anhydrosugars are mainly associated with the emissions from biomass burning during winter [e.g., (Duarte et al., 2008; Matos et al., 2017)]. The presence of a sharp resonance at  $\delta$  <sup>1</sup>H 5.3 ppm, assigned to protons bound to anomeric carbons in anhydrosugars from cellulose (Duarte et al., 2008; Matos et al., 2017), further corroborates the contribution of biomass burning into the winter WSOM samples. The occurrence of the strong H-C-O signature during summer in A Coruña may be also associated with the presence of polyols from marine oxidized organic particles (Decesari et al., 2011), although the contribution of secondary OAs formation and/or aged OAs enhanced under slightly polluted conditions cannot be ruled out (Chalbot et al., 2016; Shakya et al., 2012).

The potential contribution of fresh biomass burning emissions to winter aerosol samples can also be inferred from the aromatic content of WSOM samples collected in Aveiro (13% for  $PM_{2.5}$ ) and A Coruña (9.0% for  $PM_{2.5}$ , and 10% for  $PM_{10}$ ) as compared to those collected in summer (5.2, 2.2 and 5.9%, respectively). Also, the presence of an intense sharp resonance at  $\delta^1H$  5.3 ppm attributed to anhydrosugars in all winter samples further confirms the presence of smoke particles during this period. Interestingly, the relative content of aromatic protons in the WSOM from  $PM_{2.5}$  samples collected during summer in Aveiro is higher than those in A Coruña. A possible explanation can be related to the primary emissions from traffic sources (Heal and Hammonds, 2014), which are expectedly to be more enhanced close to the sampling site in Aveiro than in A Coruña.

Additional details on the structural differences between the aerosol WSOM samples with respect to the two suburban locations were further explored using 2D NMR spectroscopy. Figures 4 to 6 depict the  $^1H$ - $^{13}C$  HSQC NMR spectra of the WSOM samples collected in Aveiro and A Coruña during both seasons, whereas the corresponding  $^1H$ - $^{13}C$  HMBC and  $^1H$ - $^1H$  COSY NMR spectra are provided in SI (Figures S5 to S10). The HSQC NMR spectra of all WSOM samples reveal several important  $^1H$ - $^{13}C$  correlations in three major regions of chemical environments, but with very different relative intensities: aliphatic [ $\delta_H$  0.4 – 3.6 ppm /  $\delta_C$  10 – 45 ppm, represented by C-H and H-C-C= in Figure 4(B)], O-alkyl ( $\delta_H$  3.6 – 6.0 ppm /  $\delta_C$  50 – 107 ppm, including anomeric carbons), and aromatic ( $\delta_H$  6.5 – 8.5 ppm /  $\delta_C$  107 – 160 ppm) regions. The distribution of the 2D NMR cross peaks across these chemical shift areas are consistent with other 2D NMR spectral profiles found in literature related to WSOM fractions from field OAs samples (Duarte et al., 2008; Matos et al., 2017; Schmitt-Kopplin et al., 2010). By combining chemical shift information, for known organic structures (Section 2.5) and for other aerosol WSOM samples described in the literature (Duarte et al., 2008; Matos et al., 2017), with homonuclear (COSY) and heteronuclear (HSQC and HMBC) connectivity data (Figures S5 to S10), it was possible to describe the most important substructures within the WSOM components that are likely to be present in the aerosol samples collected in Aveiro and A Coruña. Figure 7 discriminates the substructures common to all WSOM samples, from those typical of each suburban location. The 2D NMR spectral assignments for each substructure are described in Table S5 (section S7), in SI.

<FIGURE 4> & <FIGURE 5> & <FIGURE 6> & <FIGURE 7>

Overall, 20 polyfunctional aliphatic and aromatic substructures (labeled as (1) to (19) in Figure 7, and Table S5 in SI) were identified in this study as being common to all aerosol WSOM samples collected in Aveiro and A Coruña. Of those, aliphatic substructures (1) to (8) were identified in both summer and winter samples, suggesting that their sources mostly remain identical in both suburban areas, regardless of the seasonal period. Such type of aliphatic substructures has been recognized as first- and/or second-generation photochemical oxidation products of different gas-phase precursors (e.g., alkanes, isoprene, carbonyl, epoxides, and anhydrides) emitted from both anthropogenic [e.g., biomass burning, fossil fuel combustion, and meat cooking (Kundu et al., 2010; Liu et al., 2011)] and natural sources [e.g., sea-to-air emission of marine organics, and terrestrial vegetation (Decesari et al., 2011; Facchini et al., 2008; Liu et al., 2011; Russell et al., 2011; Schmitt-Kopplin et al., 2012)]. For example, the persistent in both seasons and locations of molecular signatures characteristic of dimethylammonium ( $\text{DMA}^+$ ), diethylammonium ( $\text{DEA}^+$ ), and methanesulfonic acid (MSA) [substructures (5) to (7) (Figure 7 and Table S5), respectively], indicate the contribution of marine aerosols originating from the Atlantic Ocean. These three WSOM constituents are well-known tracers of marine aerosols -  $\text{DMA}^+$  and  $\text{DEA}^+$  have a biogenic oceanic source and are produced through the reaction of gaseous amines with sulfuric acid or acidic sulfates, whereas MSA is a photochemical product from marine dimethylsulfide (Facchini et al., 2008). In terms of functional group distribution, the NMR resonances assigned to these three WSOM constituents are more pronounced in the aerosol WSOM samples collected in summer with respect to those collected in winter (Figure 3). This feature is likely associated to the enhanced marine biological activity during summer as opposed to winter period, when plankton blooming is at its lowest (Cavalli et al., 2004; O'Dowd et al. 2004). The marine origin of these aerosol WSOM constituents also agree with the principal component and cluster analyses (PCA and CA, respectively) performed for major water-soluble ions and metals present in the  $\text{PM}_{2.5}$  and  $\text{PM}_{10}$  samples (Section S5, in SI), which identified a marine source dominated by ions  $\text{Na}^+$  and  $\text{Mg}^{2+}$ . On the other hand, substructure (8) (Figure 7 and Table S5), known as aliphatic methyl esters, and whose NMR resonances are more prominent in aerosol WSOM from Aveiro, could be a secondary product derived from compounds emitted by various combustion sources (Gordon et

al., 2014; Schnelle-Kreis et al., 2007). The existence of a traffic road source, dominated by elements such as Cu, Cr, Ni and V (Section S5, in SI), favors the interpretation of the secondary formation of aliphatic methyl esters from anthropogenic precursors. Photo-oxidation of gas-phase N-containing organics from traffic emissions under the presence of atmospheric OH radicals (Barnes et al., 2010; Tong et al., 2016), could also explain the presence of substructure (21) (Figure 7 and Table S5) in WSOM samples from Aveiro. In a similar fashion, the NMR resonances assigned to structure (22) (Figure 7 and Table S5) are more prominent in summer aerosol WSOM from Aveiro. This structure closely resemble those of secondary OAs derived from green leaf volatiles, which are unsaturated, oxygenated hydrocarbons emitted in large quantities by stressed plants (e.g., grass cutting or local weather changes) (Jain et al., 2014). Its presence in summer aerosol WSOM from Aveiro could be due to the occurrence of grass cutting activities, which took place during two of the sampling days in the surrounding areas.

The aerosol WSOM samples collected at both locations also exhibit the ubiquitous presence of anhydrosugars (such as levoglucosan and mannosan - structures (9) and (10), respectively, in Figure 7 and Table S5) and disaccharides (such as trehalose and maltose - structures (11) and (12), respectively, in Figure 7 and Table S5). Levoglucosan, and to a minor extent mannosan, are well-known organic molecular markers of biomass-burning emissions [(Matos et al., 2017) and references therein]. Their contribution to the aerosol WSOM load, particularly during the winter season, confirms that biomass burning for house heating is an important source of these compounds in the studied suburban OAs. Their presence in summer samples can be due to the occurrence of forest fire events in the surrounding areas during the sampling campaign. Dimeric sugars, such as maltose, has previously been identified in aerosol samples influenced by biomass burning (Matos et al., 2017; Nolte et al., 2001). The trehalose is a fungal metabolite usually referred as a tracer for the resuspension of surface soil and unpaved road dust and associated microbiota (Simoneit et al., 2004). Hence, resuspension of soil from agricultural activities in areas nearby the sampling locations could be a plausible source of this compound, particularly at A Coruña. This finding is in agreement with PCA and CA results for major water-soluble ions and metals (Section S5, in SI), which indicate the existence of a crustal source dominated by elements such as Al or  $\text{Ca}^{2+}$  or Fe. Interestingly, molecular signatures characteristic of amino sugar derivatives [structure (26), Figure 7, Table S5] were exclusively

found in both PM<sub>2.5</sub> and PM<sub>10</sub> WSOM samples collected in A Coruña, probably reflecting the contribution of fungal-derived microbial residues in resuspended soil material (Joergensen and Wichern, 2008). These results clearly indicate that soil and/or dust resuspension is an important source for aerosol WSOM at this suburban site.

Eight aromatic substructures [(13) to (20) in Figure 7] carrying neutral (aliphatic carbon), NO<sub>2</sub>, and/or oxygen-containing (namely, OCH<sub>3</sub>, OH, COOR, and COR, where R = H or alkyl group) substituents were consistently found in the aerosol samples collected at both suburban locations, particularly during the winter season. One exception is the terephthalic acid [structure (14) in Figure 7, Table S5,  $\delta_H$  8.11 /  $\delta_C$  130.4 ppm], whose NMR resonances are present in all aerosol WSOM samples, being particularly intense in summer and winter WSOM samples from Aveiro. Terephthalic acid has already been detected in urban and suburban areas, including Aveiro (Matos et al., 2017), being associated with the oxidation of aromatic hydrocarbons from urban traffic emissions (Chalbot et al., 2014; Lee et al., 2014). In a similar fashion, nitrophenyl-derived compounds [substructure (23) in Figure 7, Table S5], whose NMR resonances were exclusively found in WSOM samples from Aveiro, have been mainly attributed to traffic emissions (Tong et al., 2016). Smog chamber studies have also suggested that nitroaromatic compounds in the aerosol phase may also originate from the photo-oxidation of anthropogenic volatile organic compounds, such as toluene (Kelly et al., 2010) and benzene (Borrás et al., 2012), under different NO<sub>x</sub> concentrations. In this regard, the city of Aveiro distances 15 km from industrial sources producing aniline and nitrobenzene compounds (see Section 2.1). The photo-oxidation of gas-phase N-containing aromatics emitted from those sources cannot be excluded as an SOA source in this urban region. Overall, these findings reflect a notable influence of anthropogenic emissions to the secondary (and more water-soluble) OAs formation at Aveiro. Moreover, substructures (15) to (20) have been usually used as tracers for biomass burning emissions (Duarte et al., 2008; Matos et al., 2017). Once in the atmosphere, these structures can also undergo photooxidation, originating highly oxidized SOA species. For example, substructures (16) and (17) in Figure 7, are likely to originate from the photo-oxidation of *m*-cresol (emitted from biomass burning) in the presence of NO<sub>x</sub> (Iinuma et al., 2010). Two additional lignaceous structures [substructures (24) and (25) in Figure 7] were exclusively found in winter aerosol WSOM collected at Aveiro, thus highlighting the prominent influence of

biomass burning emissions into the aerosol WSOM characteristics, particularly at the suburban site of Aveiro.

#### 4. Conclusions

This study employed a multidimensional non-targeted analytical strategy to investigate and compare the chemical composition of water-soluble OAs from two contrasting suburban environments at the Iberian Peninsula Coast: Aveiro and A Coruña. Three major questions have guided this study: (i) how the levels of ambient water-soluble OAs distribute along this region, (ii) how they compare in terms of their structural composition and sources, and (iii) whether would be possible to complement existing OAs source profiles within this region. Parallel sampling campaigns during summer and winter seasons made it possible to conclude that:

- (1) Ambient concentrations of PM<sub>2.5</sub> and its TC, TN, and WSOC components were consistently higher in Aveiro than in A Coruña, with the highest levels of TC and WSOC being found during winter at both locations. In A Coruña, the concentrations of PM<sub>10</sub> coarse fractions were higher than those of PM<sub>2.5</sub>, especially during summer. At this site, the highest levels of TC and WSOC were comprised in PM<sub>10</sub> coarse fractions, during both seasons.
- (2) Stable isotopic  $\delta^{13}\text{C}$  and  $\delta^{15}\text{N}$  in PM<sub>2.5</sub> suggest an important contribution of anthropogenic fresh OAs at Aveiro, regardless of the seasonal period. In A Coruña, summer PM<sub>2.5</sub> and PM<sub>10</sub> samples are enriched in  $^{13}\text{C}$  and depleted in  $^{15}\text{N}$  when compared to those collected during winter, suggesting a decreased anthropogenic input at this suburban location during warmer conditions.
- (3) The EEM fluorescence profiles were very similar for all WSOM samples. However, the 1D and 2D NMR analysis confirmed differences in their structural composition, likely reflecting differences in aging processes and/or local sources between the two suburban locations. At both studied locations, the saturated (H-C) and unsaturated (H-C-C=) aliphatic structures, and oxygenated alkyls (H-C-O) accounted for most of the characterized WSOM functional groups (86-97%), with the highest content being observed during summer and the lowest during winter. The aromatic (Ar-H) content exhibited an opposite trend, with the highest values being observed during winter (9-13%) and the smallest during summer (2.2-

5.9%). Nevertheless, the relative contribution of each proton functional group differs between the two locations. For PM<sub>2.5</sub> WSOM in Aveiro, their relative contribution varies in the following order: H-C > H-C-C= > H-C-O > Ar-H. In contrast, for PM<sub>2.5</sub> and PM<sub>10</sub> WSOM in A Coruña, the relative contribution of H-C-O groups equals and/or surpasses that of H-C-C= groups, being also higher than those collected in Aveiro.

- (4) Based on 1D and 2D NMR molecular signatures, the structural composition of WSOM in PM<sub>2.5</sub> and PM<sub>10</sub> at A Coruña is dominated by oxygenated aliphatic compounds, witnessing formation or transformation processes from biogenic, marine, and soil dust precursors, with a minor influence of emissions from biomass burning, industrial, and traffic sources particularly for PM<sub>2.5</sub>. In contrast, WSOM in PM<sub>2.5</sub> at Aveiro appears to be significantly impacted by both primary and secondary anthropogenic OAs (road traffic, industry, and biomass burning emissions), exhibiting a structural composition that can be reconciled with the presence of aged polluted air. Nonetheless, the presence of molecular fingerprints typical of biogenic oceanic sources (DMA<sup>+</sup>, DEA<sup>+</sup>, and MSA) also pinpoint to the contribution of marine OAs to WSOM in Aveiro. Hence, these marine-derived molecular signatures are considerably more important in aerosol WSOM at A Coruña, during summer.

The noteworthy structural findings and source signatures reported in this study for aerosol WSOM pinpoint the need to build, in the future, a consistent assessment on the seasonal and spatial variability of the water-soluble OAs composition within and between different Iberian coastal locations. To accomplish this goal, one needs to expand this study both in time and spatial dimensions, and include other atmospheric parameters related to air quality.

## Acknowledgments

Thanks are due for the financial support to: CESAM (UID/AMB/50017 - POCI-01-0145-FEDER-007638); Organic Chemistry Research Unit (QOPNA, UID/QUI/00062/2013); FCT/MEC through national funds, Portuguese NMR network, and “Programa Operacional Potencial Humano - POPH”; FEDER within the PT2020 Partnership Agreement; and Compete 2020. FCT/MEC is

also acknowledged for an Investigator FCT Contract (IF/00798/2015). This work was also supported by Xunta de Galicia ( Programa de Consolidación y Estructuración de Unidades de Investigación Competitivas Refs. GRC2013-047 and ED431C 2017/28). João T.V. Matos and P. Esperón are greatly acknowledged for their collaboration.

## References

- Aggarwal SG, Kawamura K, Umarji GS, Tachibana E, Patil RS, Gupta PK. Organic and inorganic markers and stable C-, N-isotopic compositions of tropical coastal aerosols from megacity Mumbai: Sources of organic aerosols and atmospheric processing. *Atmos Chem Phys* 2013;13:4667–80. doi:10.5194/acp-13-4667-2013.
- Agnihotri R, Karapurkar SG, Sarma VVSS, Yadav K, Kumar MD, Sharma C, et al. Stable isotopic and chemical characteristics of bulk aerosols during winter and summer season at a station in Western Coast of India (Goa). *Aerosol Air Qual Res* 2015;15:888–900. doi:10.4209/aaqr.2014.07.0127.
- Andrade-Eiroa Á, Canle M, Cerdá V. Environmental applications of excitation-emission spectrofluorimetry: An in-depth review II. *Appl Spectrosc Rev* 2013;48:77–141. doi:10.1080/05704928.2012.692105.
- Andreae MO, Gelencsér A. Black carbon or brown carbon? The nature of light-absorbing carbonaceous aerosols. *Atmos Chem Phys* 2006;6:3419–63. doi:10.5194/acpd-6-3419-2006.
- Baghoth SA, Sharma SK, Amy GL. Tracking natural organic matter (NOM) in a drinking water treatment plant using fluorescence excitation-emission matrices and PARAFAC. *Water Res* 2011;45:797–809. doi:10.1016/j.watres.2010.09.005.
- Banfi D, Patiny L. www.nmrdb.org: Resurrecting and Processing NMR Spectra On-line. *Chim Int J Chem* 2008;62:280–1. doi:10.2533/chimia.2008.280.
- Barnes I, Solognac G, Mellouki A, Becker KH. Aspects of the Atmospheric Chemistry of Amides. *ChemPhysChem* 2010;11:3844–57. doi:10.1002/cphc.201000374.
- Bauer H, Claeys M, Vermeylen R, Schueller E, Weinke G, Berger A, et al. Arabitol and mannitol as tracers for the quantification of airborne fungal spores. *Atmos Environ* 2008;42:588–93.

doi:10.1016/j.atmosenv.2007.10.013.

Bond TC, Doherty SJ, Fahey DW, Forster PM, Berntsen T, DeAngelo BJ, et al. Bounding the role of black carbon in the climate system: A scientific assessment. *J Geophys Res Atmos* 2013;118:5380–552. doi:10.1002/jgrd.50171.

Borrás E, Tortajada-Genaro LA. Secondary organic aerosol formation from the photo-oxidation of benzene. *Atmos Environ* 2012;47:154-63. doi:10.1016/j.atmosenv.2011.11.020.

Burshtein N, Lang-Yona N, Rudich Y. Ergosterol, arabitol and mannitol as tracers for biogenic aerosols in the eastern Mediterranean. *Atmos Chem Phys* 2011;11:829–39. doi:10.5194/acp-11-829-2011.

Cavalli F, Facchini MC, Decesari S, Mircea M, Emblico L, Fuzzi S, et al. Advances in characterization of size-resolved organic matter in marine aerosol over the North Atlantic. *J Geophys Res Atmos* 2004;109:1–14. doi:10.1029/2004JD005137.

Chalbot M-CG, Brown J, Chitranshi P, Gamboa da Costa G, Pollock ED, Kavouras IG. Functional characterization of the water-soluble organic carbon of size-fractionated aerosol in the southern Mississippi Valley. *Atmos Chem Phys* 2014;14:6075–88. doi:10.5194/acp-14-6075-2014.

Chalbot M-CG, Chitranshi P, Gamboa da Costa G, Pollock E, Kavouras IG. Characterization of water-soluble organic matter in urban aerosol by <sup>1</sup>H-NMR spectroscopy. *Atmos Environ* 2016;128:235–45. doi:10.1016/j.atmosenv.2015.12.067.

Chen Q, Miyazaki Y, Kawamura K, Matsumoto K, Coburn S, Volkamer R, et al. Characterization of Chromophoric Water-Soluble Organic Matter in Urban, Forest, and Marine Aerosols by HR-ToF-AMS Analysis and Excitation-Emission Matrix Spectroscopy. *Environ Sci Technol* 2016;50:10351–60. doi:10.1021/acs.est.6b01643.

Contini D, Cesari D, Genga A, Siciliano M, Ielpo P, Guascito MR, et al. Source apportionment of size-segregated atmospheric particles based on the major water-soluble components in Lecce (Italy). *Sci Total Environ* 2014;472:248–61. doi:10.1016/j.scitotenv.2013.10.127.

Decesari S, Facchini MC, Fuzzi S, McFiggans GB, Coe H, Bower KN. The water-soluble organic component of size-segregated aerosol, cloud water and wet depositions from Jeju Island during ACE-Asia. *Atmos Environ* 2005;39:211–22. doi:10.1016/j.atmosenv.2004.09.049.

- Decesari S, Finessi E, Rinaldi M, Paglione M, Fuzzi S, Stephanou EG, et al. Primary and secondary marine organic aerosols over the North Atlantic Ocean during the MAP experiment. *J Geophys Res Atmos* 2011;116:1–21. doi:10.1029/2011JD016204.
- O'Dowd CD, Facchini MC, Cavalli F, Ceburnis D, Mircea M, Decesari S, et al. Biogenically driven organic contribution to marine aerosol. *Nature* 2004;431:676–80. doi:10.1038/nature02959.
- Duarte RMBO, Freire SMSC, Duarte AC. Investigating the water-soluble organic functionality of urban aerosols using two-dimensional correlation of solid-state <sup>13</sup>C NMR and FTIR spectral data. *Atmos Environ* 2015;116:245–52. doi:10.1016/j.atmosenv.2015.06.043.
- Duarte RMBO, Matos JT V., Paula AS, Lopes SP, Ribeiro S, Santos JF, et al. Tracing of aerosol sources in an urban environment using chemical, Sr isotope, and mineralogical characterization. *Environ Sci Pollut Res* 2017a;24:11006–16. doi:10.1007/s11356-016-7793-8.
- Duarte RMBO, Matos JTV, Paula AS, Lopes SP, Pereira G, Vasconcellos P, et al. Structural signatures of water-soluble organic aerosols in contrasting environments in South America and Western Europe. *Environ Pollut* 2017b;227:513–25. doi:10.1016/j.envpol.2017.05.011.
- Duarte RMBO, Pio CA, Duarte AC. Synchronous scan and excitation-emission matrix fluorescence spectroscopy of water-soluble organic compounds in atmospheric aerosols. *J Atmos Chem* 2004;48. doi:10.1023/B:JOCH.0000036845.82039.8c.
- Duarte RMBO, Pio CA, Duarte AC. Spectroscopic study of the water-soluble organic matter isolated from atmospheric aerosols collected under different atmospheric conditions. *Anal Chim Acta* 2005;530:7–14. doi:10.1016/j.aca.2004.08.049.
- Duarte RMBO, Santos EBH, Pio CA, Duarte AC. Comparison of structural features of water-soluble organic matter from atmospheric aerosols with those of aquatic humic substances. *Atmos Environ* 2007;41:8100–13. doi:10.1016/j.atmosenv.2007.06.034.
- Duarte RMBO, Silva AMS, Duarte AC. Two-Dimensional NMR Studies of Water-Soluble Organic Matter in Atmospheric Aerosols. *Environ Sci Technol* 2008;42:8224–30. doi:10.1021/es801298s.
- Facchini MC, Decesari S, Rinaldi M, Carbone C, Finessi E, Mircea M, et al. Important source of marine secondary organic aerosol from biogenic amines. *Environ Sci Technol*

2008;42:9116–21. doi:10.1021/es8018385.

- Fan X, Wei S, Zhu M, Song J, Peng P. Comprehensive characterization of humic-like substances in smoke PM<sub>2.5</sub> emitted from the combustion of biomass materials and fossil fuels. *Atmos Chem Phys* 2016;16:13321–40. doi:10.5194/acp-16-13321-2016.
- Fu P, Kawamura K, Chen J, Qin M, Ren L, Sun Y, et al. Fluorescent water-soluble organic aerosols in the High Arctic atmosphere. *Sci Rep* 2015;5:1–8. doi:10.1038/srep09845.
- Fu P, Kawamura K, Kobayashi M, Simoneit BRT. Seasonal variations of sugars in atmospheric particulate matter from Gosan, Jeju Island: Significant contributions of airborne pollen and Asian dust in spring. *Atmos Environ* 2012;55:234–9. doi:10.1016/j.atmosenv.2012.02.061.
- Fu PQ, Kawamura K, Pavuluri CM, Swaminathan T, Chen J. Molecular characterization of urban organic aerosol in tropical India: Contributions of primary emissions and secondary photooxidation. *Atmos Chem Phys* 2010;10:2663–89. doi:10.5194/acp-10-2663-2010.
- García-Santiago X, Gallego-Fernández N, Muniategui-Lorenzo S, Piñeiro-Iglesias M, López-Mahía P, Franco-Uría A. Integrative health risk assessment of air pollution in the northwest of Spain. *Environ Sci Pollut Res* 2017;24:3412–22. doi:10.1007/s11356-016-8094-y.
- George C, Ammann M, D'Anna B, Donaldson DJ, Nizkorodov SA. Heterogeneous photochemistry in the atmosphere. *Chem Rev* 2015;115:4218–58. doi:10.1021/cr500648z.
- Gómez-Carracedo MP, Andrade JM, Ballabio D, Prada-Rodríguez D, Muniategui-Lorenzo S, Consonni V, et al. Impact of medium-distance pollution sources in a Galician suburban site (NW Iberian peninsula). *Sci Total Environ* 2015;512–513:114–24. doi:10.1016/j.scitotenv.2015.01.029.
- Gordon TD, Presto AA, May AA, Nguyen NT, Lipsky EM, Donahue NM, et al. Secondary organic aerosol formation exceeds primary particulate matter emissions for light-duty gasoline vehicles. *Atmos Chem Phys* 2014;14:4661–78. doi:10.5194/acp-14-4661-2014.
- Graham B, Mayol-Bracero OL, Guyon P, Roberts GC, Decesari S, Facchini MC, et al. Water-soluble organic compounds in biomass burning aerosols over Amazonia 1. Characterization by NMR and GC-MS. *J Geophys Res Atmos* 2002;107. doi:10.1029/2001JD000336.
- Heal MR, Hammonds MD. Insights into the composition and sources of rural, urban and roadside carbonaceous PM<sub>10</sub>. *Environ Sci Technol* 2014;48:8995–9003.

doi:10.1021/es500871k.

Hertkorn N, Kettrup A. Molecular Level Structural Analysis of Natural Organic Matter and of Humic Substances by Multinuclear and Higher Dimensional NMR Spectroscopy. Use Humic Subst. to Remediat. Polluted Environ. From Theory to Pract., 2005, p. 391–435.

doi:10.1007/1-4020-3252-8\_21.

Iinuma Y, Böge O, Gräfe R, Herrmann H. Methyl-Nitrocatechols: Atmospheric Tracer Compounds for Biomass Burning Secondary Organic Aerosols. Environ Sci Technol 2010;44:8453–9. doi:10.1021/es102938a.

Jain S, Zahardis J, Petrucci GA. Soft ionization chemical analysis of secondary organic aerosol from green leaf volatiles emitted by turf grass. Environ Sci Technol 2014;48:4835–43. doi:10.1021/es405355d.

Joergensen RG, Wichern F. Quantitative assessment of the fungal contribution to microbial tissue in soil. Soil Biol Biochem 2008;40:2977–91. doi:10.1016/j.soilbio.2008.08.017.

Kelly JL, Michelangeli DV, Makar PA, Hastie DR, Mozurkewich M, Auld J. Aerosol speciation and mass prediction from toluene oxidation under high NO<sub>x</sub> conditions. Atmos Environ 2010;44:361–69. doi:10.1016/j.atmosenv.2009.10.035.

Kiss G, Varga B, Galambos I, Ganszky I. Characterization of water-soluble organic matter isolated from atmospheric fine aerosol. J Geophys Res Atmos 2002;107. doi:10.1029/2001JD000603.

Kundu S, Kawamura K, Andreae TW, Hoffer A, Andreae MO. Molecular distributions of dicarboxylic acids, ketocarboxylic acids and  $\alpha$ -dicarbonyls in biomass burning aerosols: implications for photochemical production and degradation in smoke layers. Atmos Chem Phys 2010;10:2209–25. doi:10.5194/acp-10-2209-2010.

Laskin A, Laskin J, Nizkorodov S. Chemistry of atmospheric brown carbon. Chem Rev 2015;115:4335–82. doi:10.1021/cr5006167.

Lee HJ, Aiona PK, Laskin A, Laskin J, Nizkorodov SA. Effect of solar radiation on the optical properties and molecular composition of laboratory proxies of atmospheric brown carbon. Environ Sci Technol 2014;48:10217–26. doi:10.1021/es502515r.

Lee HJ, Laskin A, Laskin J, Nizkorodov SA. Excitation-emission spectra and fluorescence quantum yields for fresh and aged biogenic secondary organic aerosols. Environ Sci

- Technol 2013;47:5763–70. doi:10.1021/es400644c.
- Liang L, Engling G, He K, Du Z, Cheng Y, Duan F. Evaluation of fungal spore characteristics in Beijing, China, based on molecular tracer measurements. *Environ Res Lett* 2013;8. doi:10.1088/1748-9326/8/1/014005.
- Liu S, Day DA, Shields JE, Russell LM. Ozone-driven daytime formation of secondary organic aerosol containing carboxylic acid groups and alkane groups. *Atmos Chem Phys* 2011;11:8321–41. doi:10.5194/acp-11-8321-2011.
- Lopes SP, Matos JTV, Silva AMS, Duarte AC, Duarte RMBO. <sup>1</sup>H NMR studies of water- and alkaline-soluble organic matter from fine urban atmospheric aerosols. *Atmos Environ* 2015;119:374–80. doi:10.1016/j.atmosenv.2015.08.072.
- Martin M, Tritscher T, Jurányi Z, Heringa MF, Sierau B, Weingartner E, et al. Hygroscopic properties of fresh and aged wood burning particles. *J Aerosol Sci* 2013;56:15–29. doi:10.1016/j.jaerosci.2012.08.006.
- Matos JTV, Duarte RMBO, Lopes SP, Silva AMS, Duarte AC. Persistence of urban organic aerosols composition: Decoding their structural complexity and seasonal variability. *Environ Pollut* 2017;231:281–90. doi:10.1016/j.envpol.2017.08.022.
- Matos JTV, Freire SMSC, Duarte RMBO, Duarte AC. Natural organic matter in urban aerosols: Comparison between water and alkaline soluble components using excitation–emission matrix fluorescence spectroscopy and multiway data analysis. *Atmos Environ* 2015a;102:1–10. doi:10.1016/j.atmosenv.2014.11.042.
- Matos JTV, Freire SMSC, Duarte RMBO, Duarte AC. Profiling water-soluble organic matter from urban aerosols using comprehensive two-dimensional liquid chromatography. *Aerosol Sci Technol* 2015b;49:381–89. doi: 10.1080/02786826.2015.1036394.
- Mellouki A, Wallington TJ, Chen J. Atmospheric Chemistry of Oxygenated Volatile Organic Compounds: Impacts on Air Quality and Climate. *Chem Rev* 2015;115:3984–4014. doi:10.1021/cr500549n.
- Mkoma S, Kawamura K, Tachibana E, Fu P. Stable carbon and nitrogen isotopic compositions of tropical atmospheric aerosols: sources and contribution from burning of C<sub>3</sub> and C<sub>4</sub> plants to organic aerosols. *Tellus B* 2014;1:1–14. doi:10.3402/tellusb.v66.20176.
- Mladenov N, Alados-Arboledas L, Olmo FJ, Lyamani H, Delgado A, Molina A, et al. Applications

- of optical spectroscopy and stable isotope analyses to organic aerosol source discrimination in an urban area. *Atmos Environ* 2011;45:1960–9. doi:10.1016/j.atmosenv.2011.01.029.
- Mladenov N, Reche I, Olmo FJ, Lyamani H, Alados-Arboledas L. Relationships between spectroscopic properties of high-altitude organic aerosols and Sun photometry from ground-based remote sensing. *J Geophys Res* 2010;115:G00F11. doi:10.1029/2009JG000991.
- Moise T, Flores JM, Rudich Y. Optical properties of secondary organic aerosols and their changes by chemical processes. *Chem Rev* 2015;115:4400–39. doi:10.1021/cr5005259.
- Moreda-Piñero J, Turnes-Carou I, Alonso-Rodríguez E, Moscoso-Pérez C, Blanco-Heras G, López-Mahía P, et al. The Influence of Oceanic Air Masses on Concentration of Major Ions and Trace Metals in PM<sub>2.5</sub> Fraction at a Coastal European Suburban Site. *Water Air Soil Pollut* 2015;226:2240. doi:10.1007/s11270-014-2240-2.
- Narukawa M, Kawamura K, Li S-M, Bottenheim JW. Stable carbon isotopic ratios and ionic composition of the high-Arctic aerosols: An increase in  $\delta^{13}\text{C}$  values from winter to spring. *J Geophys Res* 2008;113:D02312. doi:10.1029/2007JD008755.
- Nolte CG, Schauer JJ, Cass GR, Simoneit BRT. Highly polar organic compounds present in wood smoke and in the ambient atmosphere. *Environ Sci Technol* 2001;35:1912–9. doi:10.1021/es001420r.
- Padró LT, Tkacik D, Lathem T, Hennigan CJ, Sullivan AP, Weber RJ, et al. Investigation of cloud condensation nuclei properties and droplet growth kinetics of the water-soluble aerosol fraction in Mexico City. *J Geophys Res* 2010;115:D09204. doi:10.1029/2009JD013195.
- Park RJ, Jacob DJ, Chin M, Martin R V. Sources of carbonaceous aerosols over the United States and implications for natural visibility. *J Geophys Res* 2003;108:4355. doi:10.1029/2002JD003190.
- Pio CA, Legrand M, Oliveira T, Afonso J, Santos C, Caseiro A, et al. Climatology of aerosol composition (organic versus inorganic) at nonurban sites on a west-east transect across Europe. *J Geophys Res Atmos* 2007;112:1–15. doi:10.1029/2006JD008038.
- Pöschl U. Atmospheric aerosols: Composition, transformation, climate and health effects.

- Angew Chemie - Int Ed 2005;44:7520–40. doi:10.1002/anie.200501122.
- Putaud JP, Van Dingenen R, Alastuey A, Bauer H, Birmili W, Cyrus J, et al. A European aerosol phenomenology - 3: Physical and chemical characteristics of particulate matter from 60 rural, urban, and kerbside sites across Europe. *Atmos Environ* 2010;44:1308–20. doi:10.1016/j.atmosenv.2009.12.011.
- Querol X, Alastuey A, Pey J, Cusack M, Pérez N, Mihalopoulos N, et al. Variability in regional background aerosols within the Mediterranean. *Atmos Chem Phys* 2009;9:4575–91. doi:10.5194/acp-9-4575-2009.
- Querol X, Alastuey A, Viana M, Moreno T, Reche C, Minguillón MC, et al. Variability of carbonaceous aerosols in remote, rural, urban and industrial environments in Spain: Implications for air quality policy. *Atmos Chem Phys* 2013;13:6185–206. doi:10.5194/acp-13-6185-2013.
- Ramos AM, Nieto R, Tomé R, Gimeno L, Trigo RM, Liberato MLR, et al. Atmospheric rivers moisture sources from a Lagrangian perspective. *Earth Syst Dyn* 2016;7:371–84. doi:10.5194/esd-7-371-2016.
- Reid JS, Koppmann R, Eck TF, Eleuterio DP. A review of biomass burning emissions part II: intensive physical properties of biomass burning particles. *Atmos Chem Phys* 2005;5:799–825. doi:10.5194/acp/2005-5-799.
- Russell LM, Bahadur R, Ziemann PJ. Identifying organic aerosol sources by comparing functional group composition in chamber and atmospheric particles. *Proc Natl Acad Sci* 2011;108:3516–21. doi:10.1073/pnas.1006461108.
- Russo MA, Leitão J, Gama C, Ferreira J, Monteiro A. Shipping emissions over Europe: A state-of-the-art and comparative analysis. *Atmos Environ* 2018;177:187–94. doi:10.1016/j.atmosenv.2018.01.025.
- Saffari A, Daher N, Shafer MM, Schauer JJ, Sioutas C. Global Perspective on the Oxidative Potential of Airborne Particulate Matter: A Synthesis of Research Findings. *Environ Sci Technol* 2014;48:7576–83. doi:10.1021/es500937x.
- Salma I, Ocskay R, Chi X, Maenhaut W. Sampling artefacts, concentration and chemical composition of fine water-soluble organic carbon and humic-like substances in a continental urban atmospheric environment. *Atmos Environ* 2007;41:4106–18. doi:

10.1016/j.atmosenv.2007.01.027.

- Schmitt-Kopplin P, Gelencsér A, Dabek-Zlotorzynska E, Kiss G, Hertkorn N, Harir M, et al. Analysis of the Unresolved Organic Fraction in Atmospheric Aerosols with Ultrahigh-Resolution Mass Spectrometry and Nuclear Magnetic Resonance Spectroscopy: Organosulfates As Photochemical Smog Constituents †. *Anal Chem* 2010;82:8017–26. doi:10.1021/ac101444r.
- Schmitt-Kopplin P, Liger-Belair G, Koch BP, Flerus R, Kattner G, Harir M, et al. Dissolved organic matter in sea spray: a transfer study from marine surface water to aerosols. *Biogeosciences* 2012;9:1571–82. doi:10.5194/bg-9-1571-2012.
- Schnelle-Kreis J, Sklorz M, Orasche J, Stölzel M, Peters A, Zimmermann R. Semi volatile organic compounds in ambient PM<sub>2.5</sub>. Seasonal trends and daily resolved source contributions. *Environ Sci Technol* 2007;41:3821–8. doi:10.1021/es060666e.
- Shakya KM, Place PF, Griffin RJ, Talbot RW. Carbonaceous content and water-soluble organic functionality of atmospheric aerosols at a semi-rural New England location. *J Geophys Res Atmos* 2012;117:1–13. doi:10.1029/2011JD016113.
- Simoneit BRT, Elias VO, Kobayashi M, Kawamura K, Rushdi AI, Medeiros PM, et al. Sugars - Dominant water-soluble organic compounds in soils and characterization as tracers in atmospheric particulate matter. *Environ Sci Technol* 2004;38:5939–49. doi:10.1021/es0403099.
- Simpson AJ, Burdon J, Graham CL, Hayes MHB, Spencer N, Kingery WL. Interpretation of heteronuclear and multidimensional NMR spectroscopy of humic substances. *Eur J Soil Sci* 2001;52:495–509. doi:10.1046/j.1365-2389.2001.00402.x.
- Singh S, D'Sa EJ, Swenson EM. Chromophoric dissolved organic matter (CDOM) variability in Barataria Basin using excitation-emission matrix (EEM) fluorescence and parallel factor analysis (PARAFAC). *Sci Total Environ* 2010;408:3211–22. doi:10.1016/j.scitotenv.2010.03.044.
- Song J, He L, Peng P, Zhao J, Ma S. Chemical and Isotopic Composition of Humic-Like Substances (HULIS) in Ambient Aerosols in Guangzhou, South China. *Aerosol Sci Technol* 2012;46:533–46. doi:10.1080/02786826.2011.645956.
- Stedmon CA, Markager S, Bro R. Tracing dissolved organic matter in aquatic environments

- using a new approach to fluorescence spectroscopy. *Mar Chem* 2003;82:239–54. doi:10.1016/S0304-4203(03)00072-0.
- Sun J, Ariya PA. Atmospheric organic and bio-aerosols as cloud condensation nuclei (CCN): A review. *Atmos Environ* 2006;40:795–820. doi:10.1016/j.atmosenv.2005.05.052.
- Tong H, Kourtchev I, Pant P, Keyte IJ, O'Connor IP, Wenger JC, et al. Molecular composition of organic aerosols at urban background and road tunnel sites using ultra-high resolution mass spectrometry. *Faraday Discuss* 2016;189:51–68. doi:10.1039/C5FD00206K.
- Verma V, Fang T, Guo H, King L, Bates JT, Peltier RE, et al. Reactive oxygen species associated with water-soluble PM<sub>2.5</sub> in the southeastern United States: spatiotemporal trends and source apportionment. *Atmos Chem Phys* 2014;14:12915–30. doi:10.5194/acp-14-12915-2014.
- Viana M, López JM, Querol X, Alastuey A, García-Gacio D, Blanco-Heras G, et al. Tracers and impact of open burning of rice straw residues on PM in Eastern Spain. *Atmos Environ* 2008;42:1941–57. doi:10.1016/j.atmosenv.2007.11.012.
- Witkowska A, Lewandowska A, Falkowska LM. Parallel measurements of organic and elemental carbon dry (PM<sub>1</sub>, PM<sub>2.5</sub>) and wet (rain, snow, mixed) deposition into the Baltic Sea. *Mar Pollut Bull* 2016;104:303–12. doi:10.1016/j.marpolbul.2016.01.003.
- Witkowska A, Lewandowska AU. Water soluble organic carbon in aerosols (PM<sub>1</sub>, PM<sub>2.5</sub>, PM<sub>10</sub>) and various precipitation forms (rain, snow, mixed) over the southern Baltic Sea station. *Sci Total Environ* 2016;573:337–46. doi:10.1016/j.scitotenv.2016.08.123.
- Wonaschütz A, Coggon M, Sorooshian A, Modini R, Frossard AA, Ahlm L, et al. Hygroscopic properties of smoke-generated organic aerosol particles emitted in the marine atmosphere. *Atmos Chem Phys* 2013;13:9819–35. doi:10.5194/acp-13-9819-2013.
- Wozniak AS, Bauer JE, Dickhut RM. Characteristics of water-soluble organic carbon associated with aerosol particles in the eastern United States. *Atmos Environ* 2012;46:181–8. doi:10.1016/j.atmosenv.2011.10.001.
- Xie M, Mladenov N, Williams MW, Neff JC, Wasswa J, Hannigan MP. Water soluble organic aerosols in the Colorado Rocky Mountains, USA: Composition, sources and optical properties. *Sci Rep* 2016;6:1–12. doi:10.1038/srep39339.
- Xu L, Guo H, Weber RJ, Ng NL. Chemical Characterization of Water-Soluble Organic Aerosol in

Contrasting Rural and Urban Environments in the Southeastern United States. *Environ Sci Technol* 2017;51:78–88. doi:10.1021/acs.est.6b05002.

Zhang Q, Jimenez JL, Canagaratna MR, Allan JD, Coe H, Ulbrich I, et al. Ubiquity and dominance of oxygenated species in organic aerosols in anthropogenically-influenced Northern Hemisphere midlatitudes. *Geophys Res Lett* 2007;34. doi:10.1029/2007GL029979.

ACCEPTED MANUSCRIPT

## FIGURES CAPTIONS

- Figure 1.** Scatter plots between WSOC and TC in (a) PM<sub>2.5</sub> samples collected in Aveiro and Coruña, and (b) PM<sub>2.5</sub> and PM<sub>10</sub> samples collected just in Coruña.
- Figure 2.** Typical EEM spectra (fluorescence intensity in A.U.) of WSOM in the aerosol samples collected in Aveiro and A Coruña in summer (A) and winter (B) seasons.
- Figure 3.** Solution-state 1D <sup>1</sup>H NMR spectra of WSOM from the aerosol samples collected at A Coruña [PM<sub>2.5</sub> – (a) and (b), and PM<sub>10</sub> – (e) and (f)] and Aveiro [PM<sub>2.5</sub> – (c) and (d)] during summer (SU2016) and winter (WI2017) seasons, and (g) percentage distribution of <sup>1</sup>H NMR in each aerosol WSOM sample. Four spectral regions are identified at the bottom of spectra (d) and (f): H-C, H-C-C=, H-C-O, and Ar-H. NMR resonances assigned to DMA<sup>+</sup>, DEA<sup>+</sup>, MSA (see text for explanation of acronyms), and protons bound to anomeric carbons (O-C(H)-O) are also identified. Additional resonance signals: solvent (S) – MeOH-*d*<sub>4</sub>, and tetramethylsilane (TMS) – 0.03% (v/v).
- Figure 4.** <sup>1</sup>H-<sup>13</sup>C HSQC NMR spectra of WSOM from the PM<sub>2.5</sub> samples collected during summer (SU2016) season in A Coruña (A) and Aveiro (B), and expanded aromatic region (B1) of the spectrum of WSOM collected in Aveiro. See text for the assignments of regions defined in spectrum (B); C – carbon atom.
- Figure 5.** <sup>1</sup>H-<sup>13</sup>C HSQC NMR spectra of WSOM from the PM<sub>2.5</sub> samples collected during winter (WI2017) season in A Coruña (A) and Aveiro (B).
- Figure 6.** <sup>1</sup>H-<sup>13</sup>C HSQC NMR spectra of WSOM from the PM<sub>10</sub> samples collected during (A) summer (SU2016) and (B) winter (WI2017) seasons in A Coruña.
- Figure 7.** Aliphatic, carbohydrate and aromatic substructures identified in the aerosol WSOM samples collected in Aveiro and A Coruña. See text and Table S5 (in SI) for assignment of number labels, and the identity of aliphatic and aromatic substituents (R<sup>1</sup> to R<sup>9</sup>).

**Table 1.** Range and median values of ambient concentrations of PM, TC, TN, WSOC, total mass of particulate water-soluble organic matter (WSOM), and percentage of mass ratio between WSOM and PM at each location.

Sample	Total PM ( $\mu\text{g m}^{-3}$ )	TC ( $\mu\text{g C m}^{-3}$ )	TN ( $\mu\text{g N m}^{-3}$ )	WSOC ( $\mu\text{g C m}^{-3}$ )	WSOM <sup>(a)</sup> ( $\mu\text{g m}^{-3}$ )	WSOC/TC (%)	WS
PM <sub>2.5</sub> – SU2016	12 – 26; 14	2.5 – 4.0; 3.1	0.46 – 1.9; 0.71	0.38 – 0.82; 0.45	0.60 – 1.3; 0.71	14 – 20; 15	4.4
PM <sub>2.5</sub> – WI2017	13 – 47; 31	1.8 – 30; 6.9	0.23 – 2.5; 1.1	0.74 – 5.6; 2.8	1.2 – 8.9; 4.4	19 – 41; 39	5.9
PM <sub>2.5</sub> – SU2016	3.1 – 4.2; 3.9	0.68 – 1.5; 1.1	0.08 – 0.17; 0.14	0.06 – 0.15; 0.10	0.09 – 0.24; 0.15	8.1 – 10; 9.1	2.8
PM <sub>10</sub> – SU2016	11 – 13; 11	2.0 – 3.0; 2.6	0.28 – 0.41; 0.38	0.19 – 0.45; 0.30	0.30 – 0.72; 0.48	9.2 – 15; 12	2.6
PM <sub>2.5</sub> – WI2017	4.3 – 6.0; 5.1	0.51 – 4.1; 1.2	0.07 – 0.36; 0.16	0.13 – 0.69; 0.48	0.20 – 1.1; 0.77	17 – 46; 29	4.7
PM <sub>10</sub> – WI2017	11 – 15; 12	1.2 – 10; 3.3	0.12 – 0.97; 0.42	0.31 – 1.7; 1.2	0.50 – 2.7; 1.9	16 – 36; 31	4.7

<sup>(a)</sup> [WSOM] = [WSOC]  $\times$  1.6 (factor used to convert WSOC into WSOM derived from elemental analysis on WSOC aerosol samples collected at Aveiro (Duarte et al., 2015)).

**Table 2.** Range and median values of isotopic  $\delta^{13}\text{C}$  and  $\delta^{15}\text{N}$  composition in the fine and coarse fractions during winter and summer seasons at each location.

Location	Sample	$\delta^{13}\text{C}$ (‰)	$\delta^{15}\text{N}$ (‰)
Aveiro	PM <sub>2.5</sub> – SU2016	-28.3 to -26.7; -27.2	5.80 – 17.4; 10.8
	PM <sub>2.5</sub> – WI2017	-27.3 to -26.9; -27.0	6.87 – 11.5; 8.98
A Coruña	PM <sub>2.5</sub> – SU2016	-27.1 to -26.7; -26.9	6.29 – 7.76; 6.90
	PM <sub>10</sub> – SU2016	-26.7 to -26.5; -26.6	4.31 – 5.08; 4.86
	PM <sub>2.5</sub> – WI2017	-27.6 to -26.9; -27.2	3.12 – 14.4; 9.79
	PM <sub>10</sub> – WI2017	-27.4 to -26.9; -27.2	3.28 – 13.5; 10.0

ACCEPTED MANUSCRIPT

**HIGHLIGHTS**

- Parallel sampling of aerosol WSOM in Iberian Peninsula Coast: Aveiro vs. A Coruña
- Structural and molecular composition and major sources of WSOM in PM<sub>2.5</sub> and PM<sub>10</sub>
- Aveiro impacted by fresh & secondary anthropogenic OAs
- A Coruña impacted by secondary OAs from biogenic, soil dust & anthropogenic sources
- Marine and biomass burning OAs are also important contributors, common to both sites

ACCEPTED MANUSCRIPT

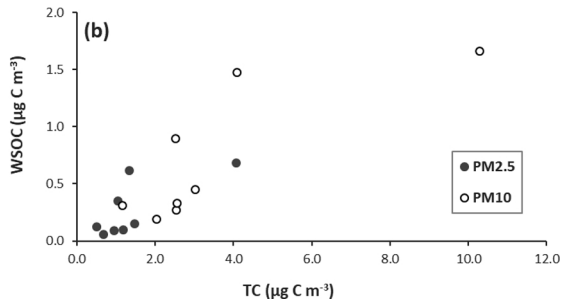
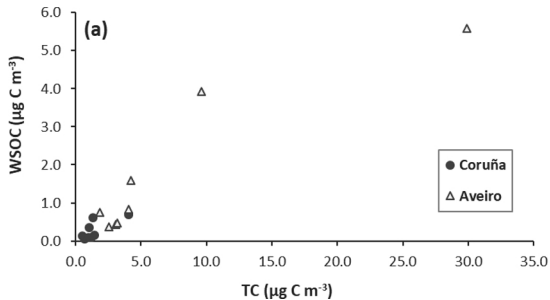
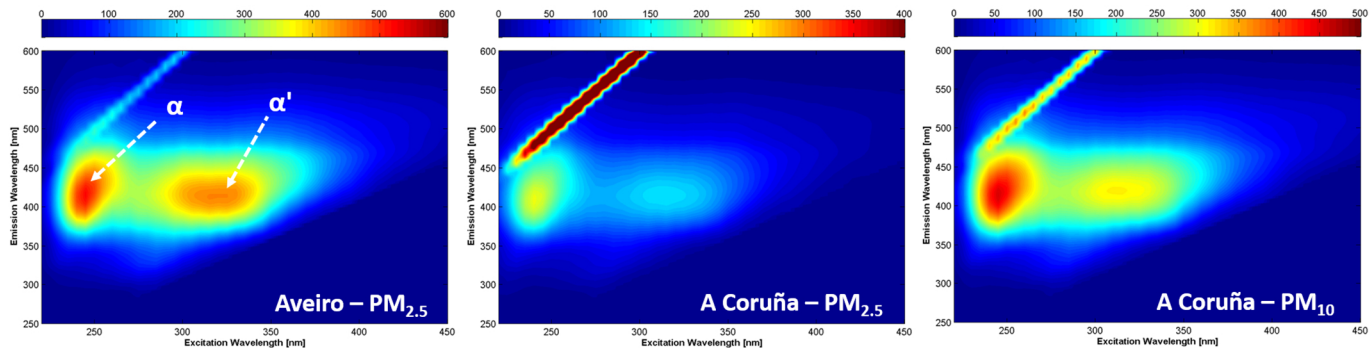


Figure 1

## (A) Summer 2016



## (B) Winter 2017

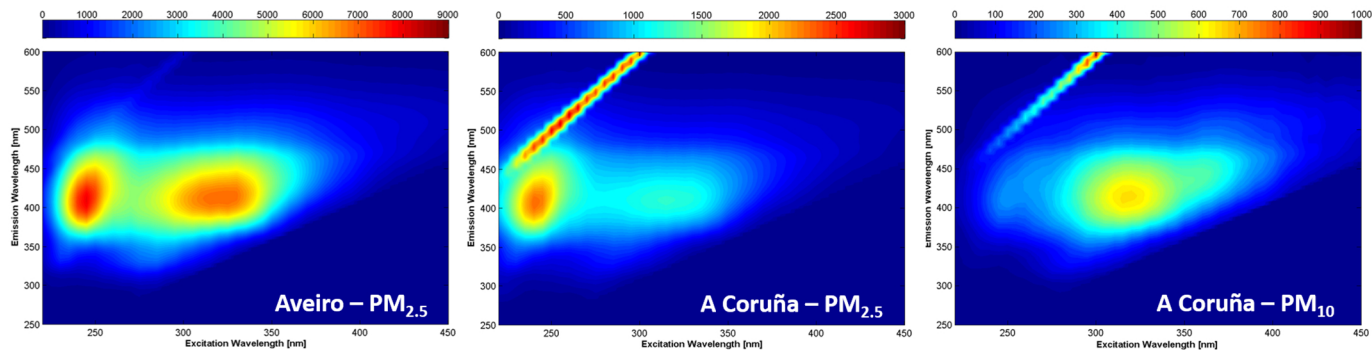


Figure 2

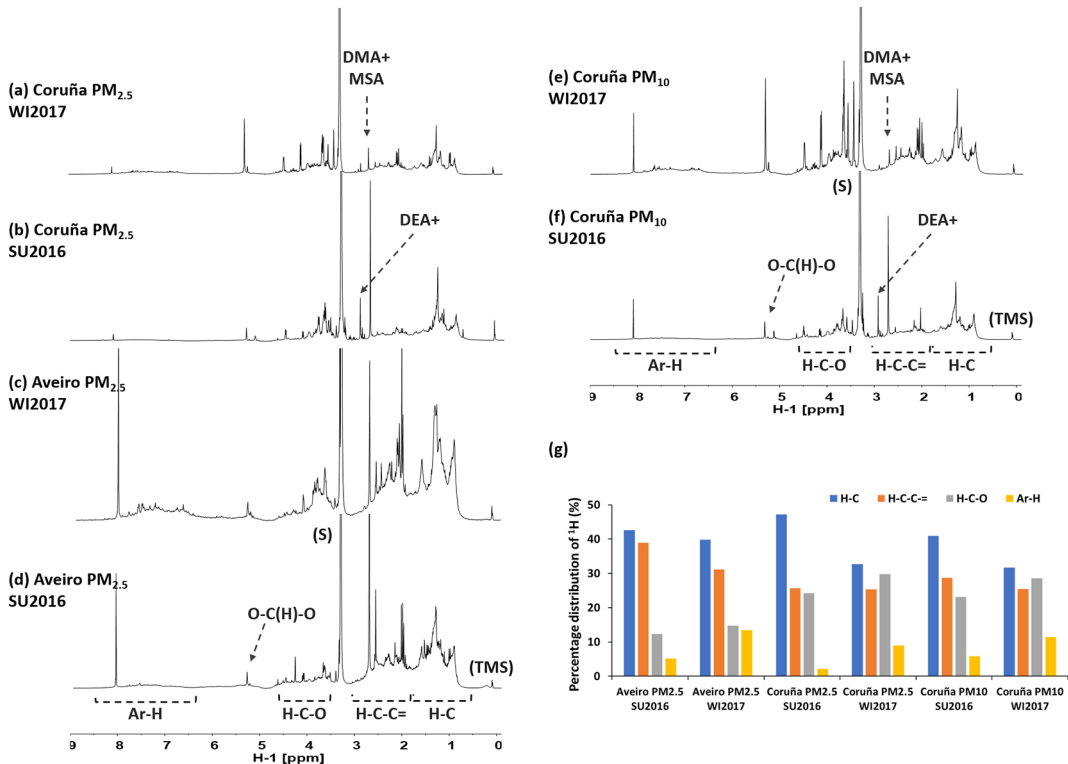


Figure 3

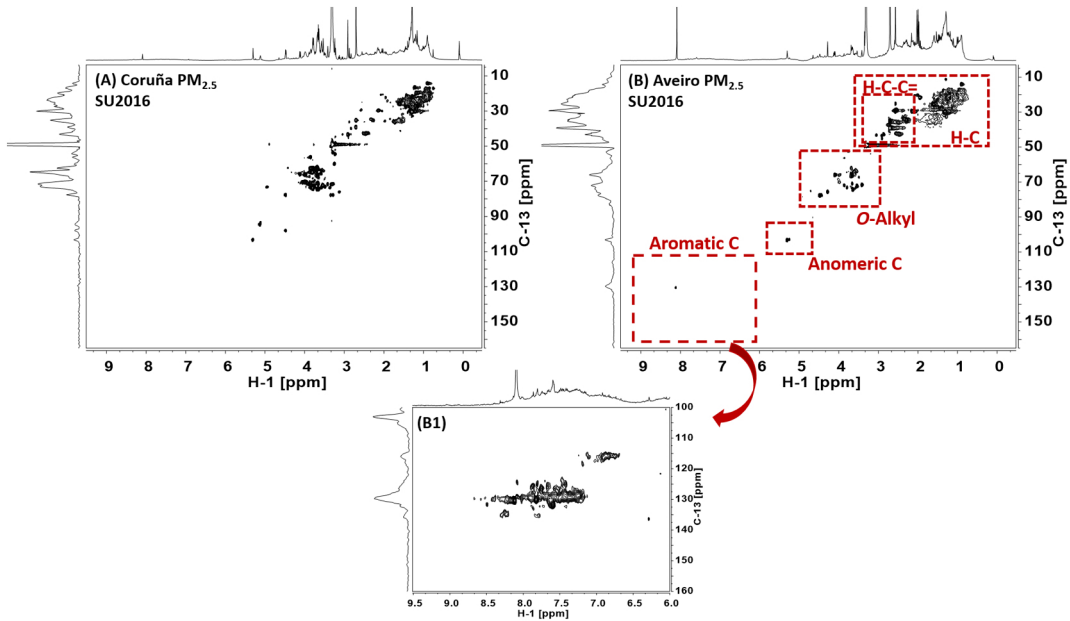


Figure 4

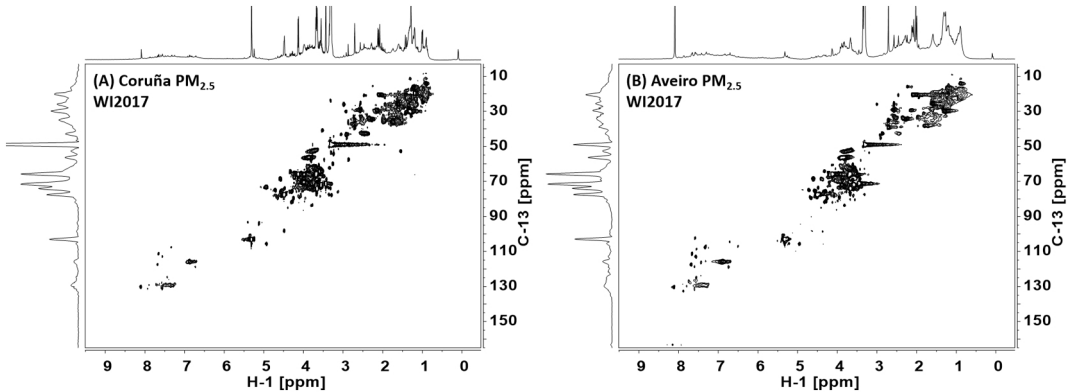


Figure 5

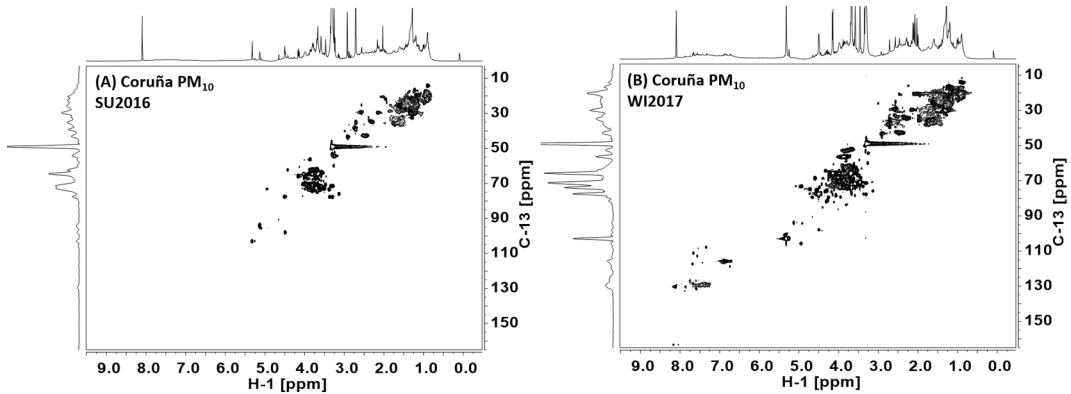
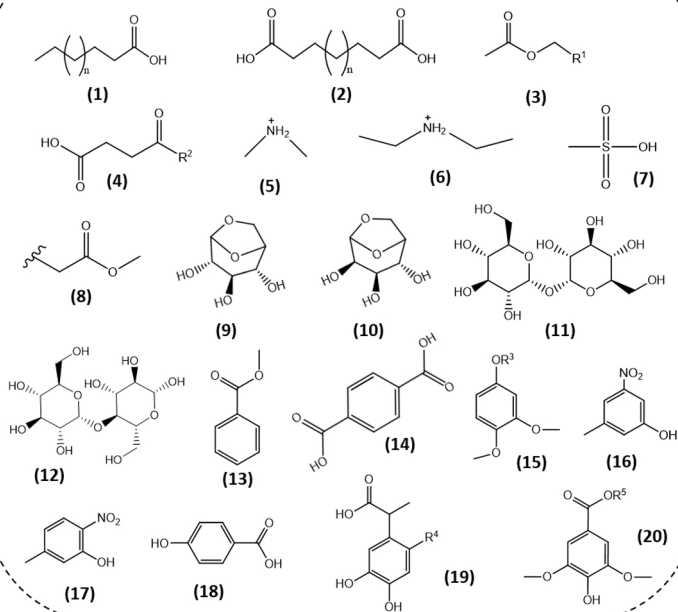
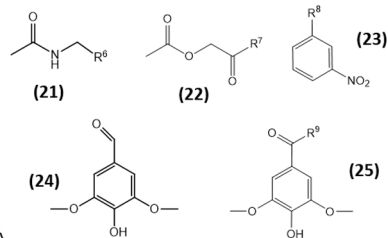


Figure 6

### Common to all PM<sub>2.5</sub> and PM<sub>10</sub> WSOM samples



### Typical of PM<sub>2.5</sub> WSOM in Aveiro



### Typical of PM<sub>2.5</sub> and PM<sub>10</sub> WSOM in A Coruña

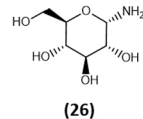


Figure 7